BMC Research Notes

RESEARCH NOTE Open Access

Functional optical coherence tomography in the study of plant-sound interactions

Uma Maheswari Rajagopalan[1*], Ryotaro Wakumoto[1], Takahiro Kono[3], Hirofumi Kadono[2] and Jun Yamada[1]

Abstract

Objective We aim to test the feasibility of applying Optical Coherence Tomography (OCT), a non-destructive, non-contact, real-time imaging technique to investigate the internal changes within leaves under sound stimulation.

Results Application of a spectral-domain OCT operating at 836.1 nm revealed that depth-resolved images obtained under no sound and under the application of sound stimuli of 100 Hz and 10 kHz sound at 100dB sound pressure to arugula (*Eruca sativa*) for a minute revealed a clear frequency dependence. The ratio of the OCT structural x-z images of a month-old arugula seedlings was obtained before and after the application of sound. From the ratio images, it was found that the effects under low and high-frequency sounds differed. The low-frequency sound of 100 Hz showed increased activity within the leaf compared to a high frequency of 10 kHz. Our results demonstrate that OCT can potentially investigate the effects of sound in plants speedily and thus has implications in agriculture applications.

Keywords Optical coherence tomography (OCT), Laser biospeckle, Scattering, Plant-sound interaction

Introduction

Water, light, carbon dioxide, temperature, and humidity are necessary for plant growth. The effects of these conditions on plant growth have been studied extensively [1], and their relationship to plant growth is becoming more evident. In recent years, sound has been attracting attention because of both positive and negative effects on plants, depending on the characteristics of the sounds. In 1973, Retallack [2] exposed plants to classical and rock music and found that classical music promoted growth. Uematsu et al. [3] reported in 2012 that continuous exposure of plants to sound increased carbon quantification and promoted growth. Gagliano et al. [4] reported that corn roots placed under 220 Hz sound showed bending of the root response in the direction of the sound source. Gagliano et al. interpreted that the roots responded to the environmental sound in search of water and actively grew towards the water flowing underground, suggesting that plants respond to natural sounds in their environment. In 2014, Appel et al. [5] demonstrated that plants could distinguish larval chewing sounds from vibrating sounds caused by other insects, such as wind and pollen; they showed that the leaves under threat showed an increased chemical reaction. The importance of acoustic communication in plants, with plants responding to sounds, has already been well established.

However, the evaluation methods used to study the plant-sound interaction require considerable time to investigate sound effects. Such methods include dry weight and yield measurements, root and stem lengths, number of tillers, and reactive oxygen species. These techniques involving several growth stages, including harvest and yield measurements, require considerable

*Correspondence:
Uma Maheswari Rajagopalan
uma@shibaura-it.ac.jp
[1]Faculty of Engineering, Shibaura Institute of Technology, 3-7-5 Toyosu, Koto-ku, Tokyo 135-8548, Japan
[2]Graduate school of Science and Engineering, Saitama University, Shimo-Okubo 255, Sakura- ku, Saitama 338-8570, Japan
[3]Tokyo Metropolitan University, Tokyo, Japan

time to estimate the effects of sound stimuli and their specific characteristics. In addition, continuous measurement and monitoring in real-time are hardly possible due to the insufficient sensitivity of the technology used. To compensate for these shortcomings, we recently proposed using the laser biospeckle method to study effects of sound on plants [6].

Laser biospeckles are formed when a sample, such as a plant leaf, is illuminated [7]. The biospeckles arise due to the interference of scattered light, with one from the surface of the leaf and the other from deep structures within the leaf. The intensity of the speckles changes randomly depending on the movement of intracellular organelles and cellular activities such as the transport of water and nutrients within the plant. By studying the dynamic change of the speckles, it is possible to monitor plant activities [8]. We used the laser biospeckle method to observe the activity of plants exposed to sound in a non-invasive, real-time manner [6]. However, such results were based on observations from the leaf's surface, and the detailed mechanisms of how sound affects the internal tissues of the leaf remain yet to be elucidated.

On the other hand, optical coherence tomography (OCT) is an interferometric technique that enables non-destructive, non-contact, real-time measurement of tomographic images of biological tissues in three dimensions. OCT has been routinely used in ophthalmology [9], dermatology and other fields [10]. Earlier, we have applied OCT to detect such function-related signals [11]. In this study, we aim to test the feasibility of the application of OCT to investigate the changes in the internal structures with exposure to sounds. For demonstration, the arugula plant was used as the sample, and its leaves were exposed to two different frequency sounds. The structural images or the OCT reflectivity signals were analyzed for the changes to sound stimuli by comparing them with those obtained without sound. A low frequency (100 Hz) and a high frequency (10 kHz) were used as sound stimuli.

Samples and experimental methods

Sample (arugula or Eruca sativa) and growth condition

Arugula is a cruciferous herb with a faint sesame-like aroma and a bitter taste. We used arugula (Eruca sativa Mill) in this study for its easy cultivation and quick growth and the seeds were purchased from Sakata seeds, Mie, Japan. The seeds were stored in a cool, dry area until use. To achieve the best germination, healthy seeds were chosen and surface sterilized. The sterilization process involved immersing the seeds in 2.5% H_2O_2 solution for 10 min, followed by three thorough rinses with distilled water.

Instead of soil, hydroponic cultivation with rockwool was used. Square cubes of rockwool (0138-008, Grotop Grodan) of sizes $3 \times 3 \times 3$ cm^3 were made by cutting and placing them in a plastic cup (100 ml). Three holes were made at the bottom of the plastic cup so that water could be sucked up from below. Then a knife was used to create a cross-shaped slit on the top of the rockwool for planting the seeds. The plastic cups were placed in a tray, and water was poured into the tray to make the rockwool absorb enough water. Two or three seeds were sown on the top of the rockwool so that the roots were less grounded to the wool. The seeds were kept in controlled chamber of constant temperature and humidity.

The nutrient medium is a mixture of commercial hydroponic fertilizers, Otsuka House No. 1 and Otsuka House No. 2, which were used to make the nutrient solution. It was obtained by diluting it with water to have an appropriate concentration and a measured electrical conductivity value (EC) of 1.0 ds/m (Gondo Electronic 7200 EC). In our preparations, 1.5 g of Otsuka House No. 1 and 1.0 g of Otsuka House No. 2 were mixed with 2.2 L of water to obtain a stock solution.

Experimental system

We used the same spectral-domain optical coherence tomography (SD-OCT) system as that used in [12], and a schematic diagram along with a sample plant and a speaker is shown in Fig. 1. A superluminescent diode (SLD) (SUPERLUM, SLD-137-HP3-DBUT-SM-PD, Cork, Ireland) with a central wavelength $\lambda_0 = 836.1$ nm and a bandwidth $\Delta\lambda = 55.2$ nm, providing a total out-power of 15.6 mW, was used as a light source. The light from the light source was first coupled to the input port of the circulator (AC Photonics, Inc., Santa Clara, CA, USA) and further divided into two beams by a 2×2 50/50 fiber coupler (TW850R5A2-2 × 2 Wideband Fiber Optic Coupler, 850 ± 100 nm, THORLABS, Exeter, UK), illuminating the sample leaf and the reference mirror, respectively. The reference arm consisted of collimating lens L1, objective lens L4, and mirror M1, and the sample arm consisted of lenses L2, L3 (LSM03-BB—Scan Lens, EFL = 36 mm, THORLABS, Exeter, UK), and Galvano scanning mirrors. Polarization controllers were used to maximize the spectral interference signal. Dispersion was compensated by a glass plate placed in front of the reference mirror, followed by offline mathematical compensation after collecting data. Light from L3 irradiated the leaf of the sample plant. The leaf was sandwiched gently between two 10 cm square magnets with a 3 cm square hole in one of them and was done to avoid minute movements during measurements. The fiber coupler recombined the backward scattered light from the leaf and the reflected light from the reference mirror M1. This light was directed through a circulator to a spectrometer that consists of a collimator, lens L5, and a grating. The collimated light illuminated the grating to obtain the spectral

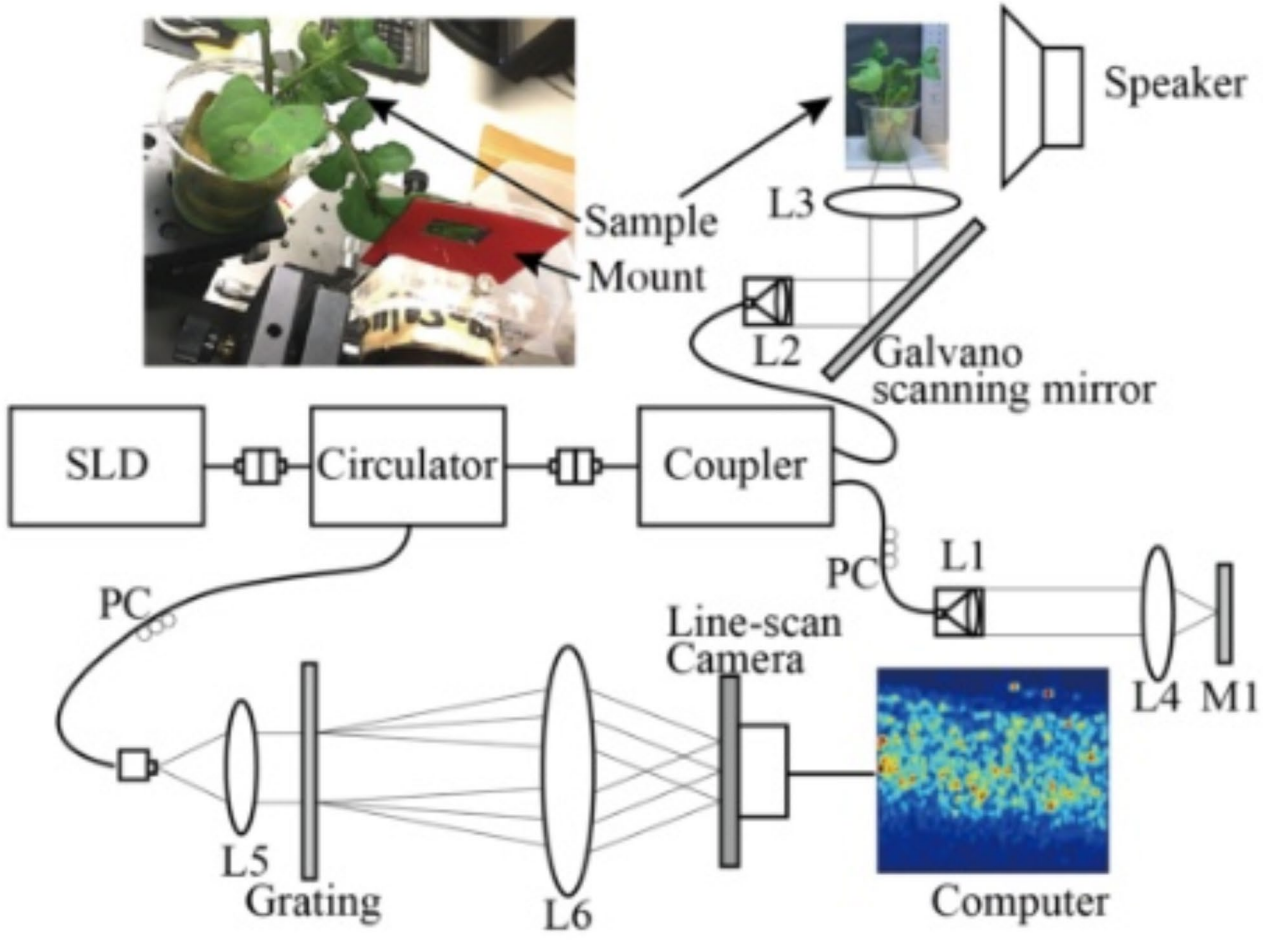

Fig. 1 A schematic of the optical system of SD-OCT with an inset of the sample holder. Here, SLD is the super luminescent diode source; L1-L6 are the lenses; M1 is the reference mirror; PC: polarization controllers. The inset shows the sample holder with the leaf of the plant mounted by sandwiching between two magnetic sheets

interference signal and was focused onto a line scan camera with 2048 pixels (L104k-2k, BASLER, Ahrensburg, Germany) through lens L6. The spectral data recorded by the camera as a function of wavelength was first mapped to frequency space and then Fourier transformed to obtain the depth variation.

Custom-built software (LABVIEW Ver.2012, National Instruments, Austin, USA) was used for acquisition and transformation to real space, and MATLAB(R2021a) was used for analyzing the images to reveal the response of the plant under exposure to sound. The power of the light incident on the leaf surface in the sample arm was 2.6 mW, which is below the irradiance damage threshold for the leaves. The two-dimensional scanning mirror (Galvano mirror scanners) can scan laterally in the X and Y directions. Each measurement is a 2048 (x) and 512 (z) raster scan over an area of 3.1×1.6 mm^2 at an acquisition rate of 10 frames per second (fps).

The depth resolution (axial resolution) of the system in free space was calculated as 6 µm using the following Eq. (1), and the lateral resolution was calculated as 22 µm by Eqs. (2),

$$\Delta z = \frac{2ln\lambda_0{}^2}{\pi\ n\Delta\lambda} \tag{1}$$

$$\Delta x = \frac{4\lambda_0}{\pi}\left[\frac{f}{d}\right] \tag{2}$$

where f is the focal length, d is the beam diameter, and n is the refractive index ($n = 1.4$).

Sound generation and exposure protocol

In order to expose the plants to sound, speakers (FOSTER, P1000-E, China) with a 10 cm full-range woofer (FOSTER, FF105WK, China) were used to produce sound. The circuit consisted of an OpAmp (TDA2030A

WINGO) to adjust the sound pressure level with a variable resistance amplifying the signal from a function generator (FG-281 TEXIO Oscillation frequency 0.01 Hz–15 MHz, Yokohama). The function generator was used to generate the required frequency. The sound pressure level was measured before starting the experiment with a sound pressure sensor (SL-100U-M INABA, Japan).

A low frequency of 100 Hz and a high frequency of 10 kHz sounds were chosen as the sound stimuli, and they were the same as the ones used in our previous experiments with laser speckles [6]. A relatively high sound pressure of 100 decibels was used to determine the possibility of structural changes within the leaf when exposed to sound. The age of the sample arugula plant was chosen to be around 30 dap (days after planting or dap), and three plants were used for the measurements. The distance between the leaf and the speaker was set to be 10 cm.

As an initial step, the arugula plants were kept in a dark and soundless environment for 60 min to eliminate the effects of ambient noise and light stimulation on the leaves. Next, the protocol shown in Fig. 2 was used to expose sound and make measurements. As of the procedure is shown in the diagram:

1. Placed for ten minutes of soundproof and no light-environment;
2. Three consecutive ten-second OCT scans were acquired at ten fps;
3. Sound exposure was given to the leaf for a period of one minute;
4. Step 2 was repeated;
5. Step 1 was repeated;
6. A total of five cycles of measurements was performed;
7. The whole procedure was repeated for three plants.

A total of 500 scans were obtained for each plant under each sound stimuli, namely no sound or control, 100 Hz, and 10 kHz. In the analysis, we calculated the ratio of the average intensity obtained during the presence of the sound to that obtained under the absence of the sound. First, the standardization per frame was done using Eq. (3), where $x_{i,j}$ is the intensity at the pixel i and j, and $\bar{x}$ was the average of all the pixel intensities in the

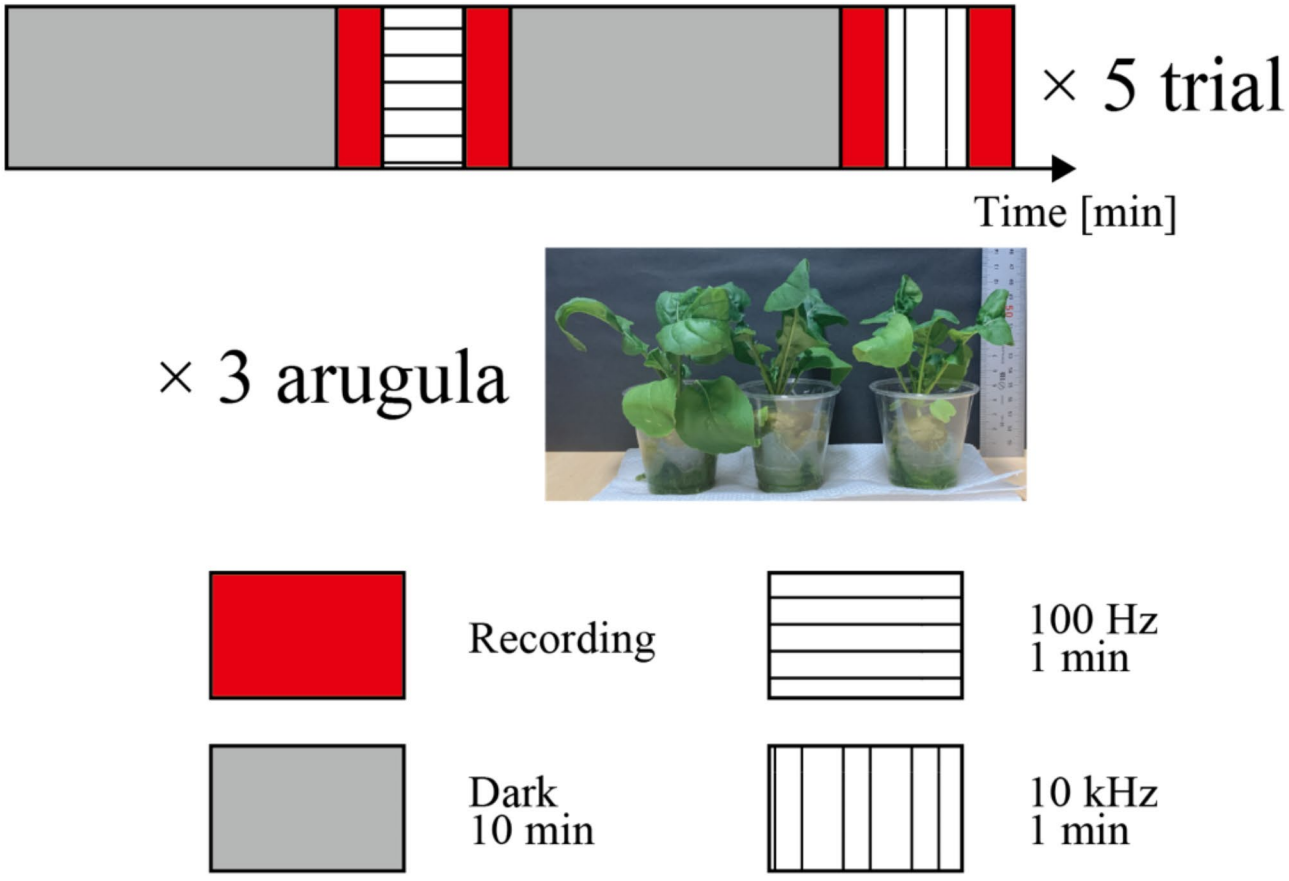

Fig. 2 Experimental protocol with three different sample plants and the conditions used. Grey and red indicate the dark and recording periods; Horizontal and vertical hatch respectively, represent 100 Hz and 10 kHz sound stimuli that were given for a minute and sequentially presented to the plant

frame. Each frame was normalized by the maximum of that frame, x_{max}.

$$x^{norm} = \frac{x_{i,j} - \bar{x}}{x_{\max} - \bar{x}} \tag{3}$$

Then, from the normalized frames x^{norm}, the average across the number of frames was obtained by the equation, Eq. (4), as given below,

$$\bar{X} = \frac{1}{N_f} \sum_{i_f=1}^{N_f} x_{i_f}^{norm} \tag{4}$$

Where i_f and N_f are, respectively, the frame number and the total number of frames.

Next, the ratio of the normalized value obtained after the exposure of sound to that obtained before exposure to sound, as given below for each trial, was calculated. This was then averaged in Eq. (5), where t is the trial number. A total of five trials were done in this study. When the ratio is larger than unity, there is a more significant change within the leaf due to sound. In the functional or ratio images, red represents a larger change, while blue represents a lower change. These signals are functional OCT or fOCT signals [11].

$$ratio = \frac{1}{N_t} \sum_{i_t=1}^{N_t} \frac{\bar{X}_{i_t}^{after}}{\bar{X}_{i_t}^{before}} \tag{5}$$

Results and discussion

Figure 3A shows the OCT structural images of the leaf under control or no sound condition from three different plants. Here, horizontal corresponds to the lateral position, and vertical corresponds to the depth. In the images shown, a layered organization across depth could be recognized with light and dark regions corresponding to higher and lower reflectivity from within the leaf layer structures.

With the sequence of images obtained for each sample, the ratio images were calculated by using Eq. 5 for each of the samples and given as pseudocolor-coded images for sound frequency of 100 Hz (top) and 10 kHz (bottom) in Fig. 3B. In the functional or ratio images, red represents a larger ratio change while blue represents a lower change. As can be seen in both under 100 Hz and 10 kHz, the surface region is almost not active, while significant differences exist in the activation patterns in the deeper region. Further, for all the sample plants used, for 100 Hz, there is more red region compared to the blue region. In contrast, for 10 kHz, there is more blue region across the depth. These results suggest that the different frequencies produce differing effects on the plant's internal structures.

For comparison, we calculated ratio images under the condition of no sound or control. Two representative examples are given as supplementary information (Figure S1). Ratio images calculated from measured OCT reflectivities under rock and classical musical stimuli (Figure S2) were found to further demonstrate the sensitivity of OCT in detecting sound-related changes across the depth of the leaf.

Our results suggest that even one-minute exposure to sound can produce structural changes in deeper regions of the leaf. Our earlier study with confocal microscopy revealed structural changes such as stomatal size changes [6]. Moreover, laser biospeckles differed depending on the frequencies, but because of the use of a camera, it collected total light from both the surface and over a range of depths and could not distinguish reflections from different depths [6].

Our results mean size changes could lead to scattering changes, which would be reflected in the ratio of fOCT or ratio signals. As the sizes of stomata get smaller at higher frequencies, it is natural to expect smaller stomata for 10 kHz than for 100 Hz. Considering the Mie scattering regime, a smaller size will lead to larger forward scattering and less backward scattering. In OCT, the light incidents normal to the sample surface, and back-reflected light from it is detected. Therefore, when there is more forward scattering within the sample, there will be less light scattered backwards, and hence, there will be less light than before sound exposure. Thus, exposure to high frequency sound will result in a lesser OCT reflectivity signal. Such a decrease in reflectivity could be the reason for the reduction of less activation or changes in the fOCT maps for 10 kHz in comparison to 100 Hz, as seen in Fig. 3B.

We want to emphasize that in OCT, because of the coherence gate employed as determined by the coherence properties of the source used, the light reflected from the surface and from specific depths could be distinguished. The depth-resolution is determined by the coherence properties of the source. In our case, it is around a few tens of micrometers. On the other hand, with laser biospeckles, our earlier work [6], they are not only due to the interference of scattered light from the surface scattering but also due to the scattered light from deeper structures and thus do not contain any depth-specific information. Moreover, while laser biospeckle is easy to implement, requiring only a laser source and a CMOS camera, OCT is a complex method consisting of an interferometer requiring sophisticated components such as a special source, fiber components, and, in this case, an expensive spectral camera.

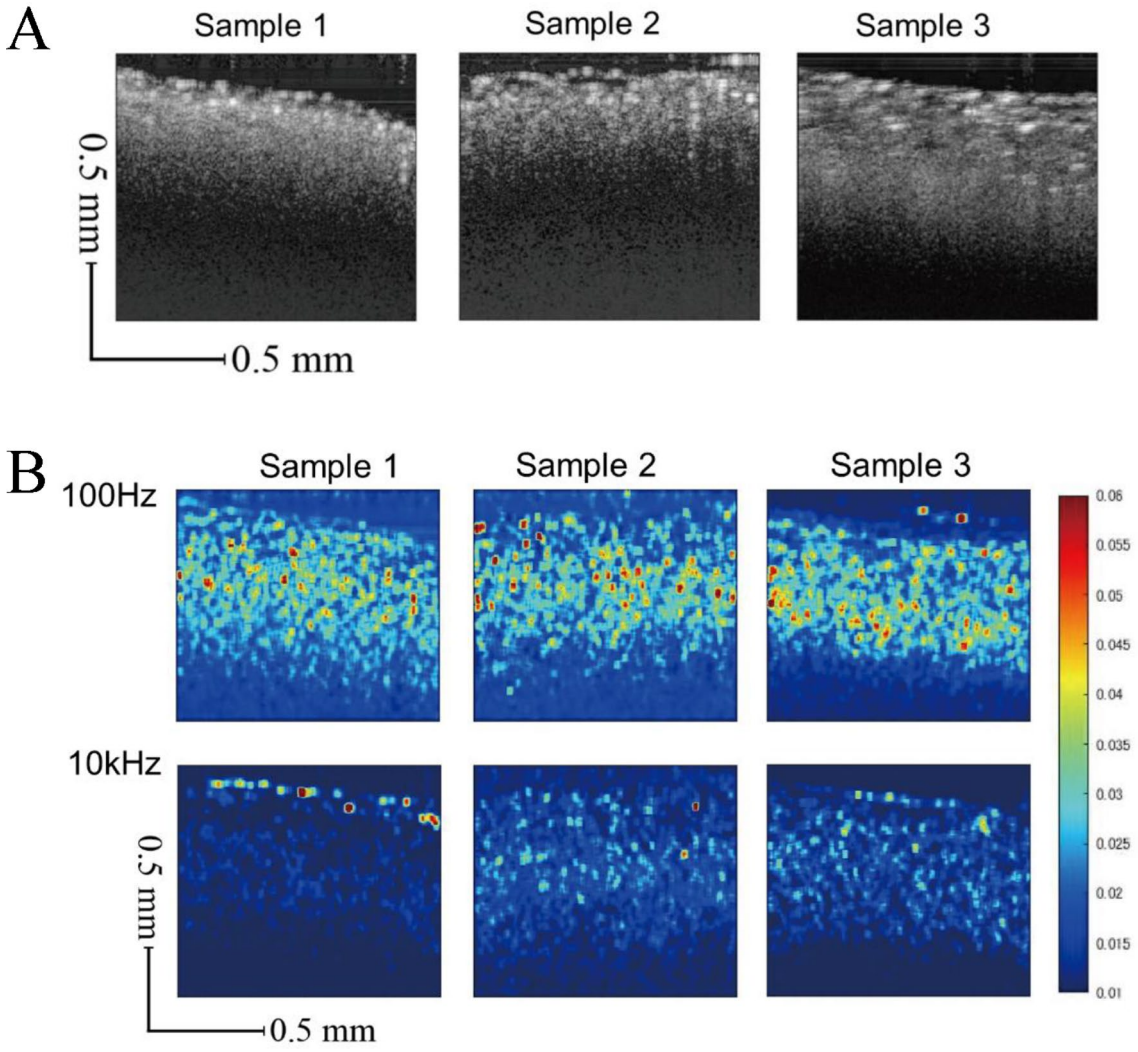

Fig. 3 (**A**). OCT structural images (x-z) of a one-month-old leaves obtained for three different samples obtained under control or no sound. As can be seen, the laminar organization of the leaf could be recognized. Bright and dark regions correspond respectively to high and low reflectivity regions. (**B**) fOCT images calculated as the ratio from the OCT images obtained after the sound to that image obtained before by Eq. 5 for each of the samples shown in Fig. 3A. Here two different frequencies, 100 Hz (top row) and 10 kHz (bottom row) are shown. Colorbar on the right corresponds to the strength of the internal changes due to the sound with red representing large changes while blue corresponds to smaller changes. As seen, high frequency containing more blue region has the effect of reducing internal activity in comparison to low-frequency sounds. For both frequencies, the ratio was obtained with respect to the no-sound condition

OCT has been widely used as a clinical tool in the diagnosis of ocular diseases. Its potential has also been demonstrated in functional studies that employ the speckles in OCT or biospeckle OCT in studying the temporal fluctuations in the study of plants [12–17]. To our knowledge, the application of OCT to visualize structural changes within plant anatomical structures in vivo is demonstrated for the first time in our study. We examined the effects of two types of sound, low frequency (100 Hz) and high frequency (10 kHz) and found that the frequency of the sound affected the OCT reflectivity with increased effects seen for lower frequency than that of high frequency. The study is preliminary, and it demonstrates the potential of OCT investigating the effects of sound on plants in vivo and that too within a short time of a few minutes.

Limitations

Despite the demonstration of the application of OCT to the study of the effects of sound on plants, OCT is a complex technique requiring sophisticated elements for building the system. We expect our study to increase the potential of OCT in the field of plant photonics, too.

Figures in S1 show examples of ratio images obtained under no sound or control. The ratio images were calculated as the ratio of OCT signals obtained under no sound; therefore, no changes should be observed. As can be seen, there was only some activity at the surface,

which is prone to high noise levels. Other than that there were no changes could be observed across the depth of the leaf demonstrating the sensitivity of the functional OCT in plant studies.

Results obtained with rock and classical music are given in Figure S2. The images were obtained from the rear side of the arugula leaf, which is supposed to contain more stomata. Stomata are believed to change during the sound stimuli, as demonstrated in our previous work [6]. For rock music, 'The Jimi Hendrix Experience - Purple Haze' was used. As classical music, Mozart's Eine kleine Nachtmusik (Karajan Vienna Philharmony recording of 1949) was used. The sound pressure level was set to 100dB for both cases. The top and bottom rows of images correspond, respectively, to classical and rock music. The leftmost, middle, and rightmost in both rows correspond to before, after, and ratio images, respectively.

For classical music, there is more uniform variation across the depth, while for rock music, there was a general reduction. Red Encircled regions show representative stomata and its variation in size with respect to different musical sounds. These results further demonstrate the effectiveness of functional OCT in sound studies in plants.

Supplementary Information

The online version contains supplementary material available at https://doi.org/10.1186/s13104-025-07131-4.

Supplementary Materials 1 and 2

Acknowledgements
Not applicable.

Author contributions
RU planned the experimental protocol and the overall guidance for the project and wrote the manuscript. RW performed the experiments, helped the analysis and prepared the figures. TK, HK and JY provided the total intellectual support and guidance in conducting the experiments and the writing up of the manuscript. All authors read and approved the final manuscript.

Funding
Not applicable.

Data availability
The datasets collected and analyzed during the current study are available from the corresponding author on reasonable request.

Declarations

Ethics approval and consent to participate
Not applicable.

Consent for publication
Not applicable.

Competing interests
The authors declare no competing interests.

Received: 26 May 2024 / Accepted: 29 January 2025
Published online: 13 February 2025

References

1. Taiz L, Zeiger E. [Plant physiology 3rd edition]. Sunderland: Sinauer Associates; 2002.
2. Dorothy LR. [The sound of Music and Plants]. Devorss&Co. 1973:1–96.
3. Uematsu K, Suzuki N, Iwamae T, Inui M, Yukawa H. Increased fructose 1,6-bisphotsphate aldolase in plastids enhances growth and photosynthesis of tobacco plants. J Exp Bot. 2012;63(8):3001–9. https://doi.org/10.1093/jxb/ers004]
4. Gagliano M, Mancuso S, Robert D. Towards understanding plant bioacoustics. Trends Plant Sci. 2012;17(6):323–5. https://doi.org/10.1016/j.tplants.2012.03.002]
5. Appel HM, Cocroft RB. Plants respond to leaf vibrations caused by insect herbivore chewing. Oecologia. 2014;175(4):1257–66. https://doi.org/10.1007/BF00984895]
6. Rajagopalan UM, et al. Demonstration of laser biospeckle method for speedy in vivo evaluation of plant-sound interactions with arugula. PLoS ONE. 2021. https://doi.org/10.1371/journal.pone.0258973]
7. Aizu Y et al. Bio-speckles. Trends Opt. 1996;3:27–49.
8. Zdunek A, et al. The Biospeckle Method for the investigation of agricultural crops: a review. Opt Lasers Eng. 2014;52:276–85. https://doi.org/10.1016/j.optlaseng.2013.06.017]
9. Huang D. Optical coherence tomography. Science. 1991;254(5035):1178–81. https://doi.org/10.1126/science.1957169]
10. Drexler W, et al. Optical coherence tomography today: speed, contrast, and multimodality. J Biomed Opt. 2014;19(7). https://doi.org/10.1117/1.JBO.19.7.071412]
11. Maheswari RU, Takaoka H, Kadono H, Homma R, Tanifuji M. Novel functional imaging technique from Brain Surface with Optical Coherence Tomography enabling visualization of depth resolved functional structure in vivo. J Neurosci Methods. 2003. https://doi.org/10.1016/S0165-0270(02)00370-9
12. Srimal LKT, Rajagopalan UM, Kadono H. Functional optical coherence tomography (fOCT) biospeckle imaging to investigate response of plant leaves to ultra-short term exposure of ozone. J Phys Conf Ser. 2015;605(1):12013. https://doi.org/10.1088/1742-6596/605/1/012013
13. Lim Y, Funada K, Kadono H. Monitor biological activities in seed germination by biospeckle optical coherence tomography. Proc SPIE. 2019;10877:108770B. https://doi.org/10.1117/12.2509725
14. Rajagopalan UM, Kabir M, Lim Y, Kadono H. Biospeckle optical coherence tomography in speedy visualizing effects of foliar application of plant growth hormone to Chinese chives leaves. BMC Res Notes. 2020;13:1–6. [CrossRef].
15. De Silva YSK, Rajagopalan UM, Kadono H, Li D. The positive and negative phenotyping of increasing Zn concentrations by Biospeckle Optical Coherence Tomography in speedy monitoring on lentil (Lens culinaris) seed germination and seedling growth. Plant Stress. 2021;2:100041. [CrossRef].
16. Danyang L, Rajagopalan UM, De Silva YSK, et al. Biospeckle Optical Coherence Tomography (bOCT) in the Speedy Assessment of the responses of the seeds of Raphanus sativus L. (Kaiware Daikon) to Acid Mine Drainage (AMD). Appl Sci. 2022;12(1):355. https://doi.org/10.3390/app12010355]
17. Li D, Rajagopalan UM, De Silva YSK, Liu F. and Hirofumi Kadono. 2022. Biospeckle Optical Coherence Tomography (bOCT) in the Speedy Assessment of the Responses of the Seeds of *Raphanus sativus* L. (Kaiware Daikon) to Acid Mine Drainage (AMD) *Applied Sciences* 12, no. 1: 355. https://doi.org/10.3390/app12010355

Publisher's note